

The Nose–Hoover thermostat

D. J. Evans and B. L. Holian

Citation: *The Journal of Chemical Physics* **83**, 4069 (1985); doi: 10.1063/1.449071

View online: <http://dx.doi.org/10.1063/1.449071>

View Table of Contents: <http://scitation.aip.org/content/aip/journal/jcp/83/8?ver=pdfcov>

Published by the **AIP Publishing**

Articles you may be interested in

[The Nosé–Hoover looped chain thermostat for low temperature thawed Gaussian wave-packet dynamics](#)
J. Chem. Phys. **140**, 194106 (2014); 10.1063/1.4875517

[Decomposition-order effects of time integrator on ensemble averages for the Nosé–Hoover thermostat](#)
J. Chem. Phys. **139**, 064103 (2013); 10.1063/1.4817194

[Crooks equation for steered molecular dynamics using a Nosé–Hoover thermostat](#)
J. Chem. Phys. **125**, 164101 (2006); 10.1063/1.2360273

[Solving the Nosé–Hoover thermostat for Nuclear Pasta](#)
AIP Conf. Proc. **841**, 558 (2006); 10.1063/1.2218236

[A configurational temperature Nosé–Hoover thermostat](#)
J. Chem. Phys. **123**, 134101 (2005); 10.1063/1.2013227



The Nose-Hoover thermostat

Denis J. Evans and Brad Lee Holian^{a)}

Research School of Chemistry, Australian National University, G.P.O. Box 4, Canberra, ACT. 2601, Australia

(Received 4 June 1985; accepted 10 July 1985)

We derive equilibrium fluctuation expressions for the linear response of many body systems thermostated by the Nose-Hoover thermostat. We show that in the thermodynamic limit this response is the same as that of the corresponding Gaussian isothermal system. Numerical comparisons for shear flow show that the calculated shear viscosity coefficient is remarkably independent of thermostating method.

I. INTRODUCTION

Recently there have been revolutionary developments in molecular dynamics methodology. In its 30 year history the molecular dynamics technique has remained almost unchanged. Newton's equations of motion are solved for a system of particles subject to periodic boundary conditions. Time averages for such a system represent fairly closely microcanonical ensemble averages. The microcanonical ensemble is however very inconvenient both for theoretical analysis and also for comparisons of computed results with experimental data. By comparison it was appreciated fairly early that Monte Carlo simulations could be performed in a wide variety of more useful ensembles. At the time it was generally thought that if one was interested in the equilibrium properties of a system where the pressure, enthalpy, or temperature (rather than the energy) were the preferred state variables, then one had no choice but to use Monte Carlo techniques.

Of course people had been cheating for some time. Many people rescaled the second moment of the atomic velocities to control the temperature of their molecular dynamic simulations.^{1,2} Moreover the results of these *ad hoc* rescaling algorithms produced reliable results provided the timesteps used were sufficiently short. In 1981 Anderson developed a hybrid Monte Carlo molecular dynamics algorithm³ which was capable of generating both the canonical and isothermal/isobaric ensembles. The stochastic nature of the Andersen algorithms made them difficult to analyze theoretically—particularly for dynamical properties.

In the meantime a number of workers had been using molecular dynamics to simulate nonequilibrium systems including nonequilibrium steady states. For these problems, standard molecular dynamics was more than merely inconvenient, it was incapable of creating homogeneous nonequilibrium steady states. The solution to this far more difficult problem was found simultaneously and independently by Hoover and Evans.^{2,4} Their solution was to rewrite the equations of classical mechanics so that thermodynamic variables other than the energy, were constants of the motion. These methods are deterministic, simple to implement and

analyze theoretically, and they work equally well for equilibrium and nonequilibrium systems. These methods are often called Gaussian methods since Gauss' Principle of Least Constraint can often be used to generate the equations of motion.

Recently a number of alternative methods have been proposed. The "momentum scaling" technique proposed by Haile and Gupta cannot thermostat nonequilibrium systems and even for equilibrium systems it contains a number of difficulties.^{5,6} The recent algorithm proposed by Berendsen⁷ is difficult to analyze theoretically since the Berendsen equations of motion are *not* time reversible.

In this paper we analyze some of the properties of a dynamics originally proposed by Nose.^{8,9} In their original form these equations were very cumbersome to implement in actual molecular dynamics computer programs. Hoover¹⁰ has recently cast Nose's equations in a form which is closely related to the Gaussian schemes mentioned earlier.

The principle differences between Nose-Hoover (NH) dynamics and the earlier Gaussian schemes is that NH dynamics allows fluctuations in the state variables whereas the Gaussian schemes rigidly clamp these variables. To date all analysis of the NH equations has been confined to their equilibrium properties. In this paper we will consider the dynamical implications of the NH equations.

II. NOSE-HOOVER DYNAMICS

We will present a short outline of the Nose equations of motion and their transformation to the more useful noncanonical Nose-Hoover form. We believe that some of the crucial points of this derivation have not been very explicit in previous discussions.

Consider the Nose Hamiltonian H_N ,

$$H_N = H_0(q, p/s) + gkT \ln s + (p_s^2/2Q), \quad (1)$$

where H_0 is the usual Hamiltonian for a classical many body system except that everywhere one would normally expect to see a momentum p appearing, it is replaced by p/s . Thus

$$H_0(q, p/s) = \sum (p_i/s)^2/2m + \Phi(q). \quad (2)$$

The microcanonical ensemble for such a system is described by the partition function

$$Z = \int dq dp dp_s ds \delta(H_N - E) \quad (3)$$

^{a)}Permanent address: MS B221, Los Alamos National Laboratory, Los Alamos, New Mexico 87545.

and the probability that the system will be observed at a particular point in phase space dq, dp, dp_s, ds , will be uniform provided that the Nose Hamiltonian takes the specified value E .

The Nose equations of motion are

$$\begin{aligned}\dot{\mathbf{q}}_i &= \mathbf{p}_i/m, \\ \dot{\mathbf{p}}_i &= \mathbf{F}_i, \\ \dot{s} &= p_s/Q, \\ \dot{p}_s &= \sum \frac{p_i^2}{ms^3} - \frac{gkT}{s}.\end{aligned}\quad (4)$$

Hoover has recently shown that these equations can be cast in a simpler, more easily understood form by transforming to the scaled momentum

$$\mathbf{p}'_i = \mathbf{p}_i/s \quad (5)$$

and to scaled time

$$t' = \int_0^t dt/s. \quad (6)$$

This same transformation had been used by Nose. However he did not take full advantage of the resulting simplifications to the equations of motion.

We should also point out that both Nose and Hoover transformed p_s to $p'_s = p_s/s$. However as we shall see this additional transformation is an unnecessary complexity. With this minor difference in mind we shall define a friction constant ξ ,

$$\xi = p_s/Q. \quad (7)$$

In scaled momentum p' and scaled time t' the equations of motion become

$$\begin{aligned}d\mathbf{q}_i/dt' &= \mathbf{p}'_i/m, \\ d\mathbf{p}'_i/dt' &= \mathbf{F}_i - \xi \mathbf{p}'_i, \\ \frac{d\xi}{dt'} &= \frac{1}{Q} \left[\sum \frac{p_i'^2}{m} - gkT \right]\end{aligned}\quad (8)$$

with the subsidiary equation of motion for s (if needed) which is

$$ds/dt' = \xi s. \quad (9)$$

Equation (9) is subsidiary to (8) since it is not needed to compute the trajectories of the N interacting particles. We shall refer to Eqs. (8) as the Nose-Hoover (NH) equations of motion.

We must emphasize that the introduction of "scaled time" t' , has important and unusual implications for the statistical mechanical relationships of the Nose and NH systems. The meaning of scaled time can be better understood by considering the transformation of propagators in the two dynamical systems. The propagator of phase variables in NH dynamics is

$$e^{iL't'} = \exp_R \int_0^{t'} \frac{iL'}{s} dt, \quad (10)$$

where \exp_R is the time ordered exponential with latest times to the right [see the discussion in Ref. 10(a)]. From Eqs. (8)

$$\begin{aligned}\frac{iL'}{s} &= \frac{1}{s} \left[\frac{\mathbf{p}'_i}{m} \cdot \frac{\partial}{\partial \mathbf{q}_i} + (\mathbf{F}_i - \xi \mathbf{p}'_i) \cdot \frac{\partial}{\partial \mathbf{p}'_i} \right. \\ &\quad \left. + s\xi \frac{\partial}{\partial s} + \left(\sum \frac{p_i'^2}{m} - gkT \right) \frac{\partial}{\partial p'_s} \right].\end{aligned}\quad (11)$$

Using Eqs. (5), (6), and (7) and the fact that

$$\left(\frac{\partial}{\partial s} \right)_{p'} = \left(\frac{\partial}{\partial s} \right)_p + \mathbf{p}'_i \cdot \frac{\partial}{\partial \mathbf{p}_i}, \quad (12)$$

we find that

$$iL'/s = iL. \quad (13)$$

Substituting into the equation for the propagator [Eq. (10)] we see that the NH p propagator is identical to the corresponding Nose propagator

$$e^{iL't'} = e^{iLt}. \quad (14)$$

Trajectories under NH and Nose dynamics follow the same paths but they traverse these paths at different (nonuniform) rates. Scaled time trajectories viewed from the perspective of Nose dynamics, evolve under non-Galilean time. This has important consequences for evaluating the full NH partition function.

To evaluate the new partition function we will first transform to the scaled momentum \mathbf{p}'_i leaving time in its original Nose (Galilean) form. The Nose partition function for a three-dimensional system becomes

$$Z = \int dq dp' dp_s ds s^{3N} \delta(H_N - E). \quad (15)$$

We will now consider the transformation to non-Galilean time. Although we are at this stage only concerned with time independent, equilibrium distribution functions the effect of introducing non-Galilean transformations of time is most easily seen by considering its influence on an equilibrium time average. If $\langle \rangle'$ denotes an equilibrium t' -time average then as Nose pointed out,⁸

$$\langle A \rangle' = \frac{1}{T'} \int_0^{T'} dt' A(t'). \quad (16)$$

Using Eq. (6) this becomes

$$\langle A \rangle' = \frac{\int_0^T dt A(t)/s}{\int_0^T dt/s}. \quad (17)$$

However since the propagators are identical [Eq. (14)], we find that

$$\langle A \rangle' = \langle A/s \rangle / \langle 1/s \rangle. \quad (18)$$

Equation (18) shows that the partition function in scaled time Z' must be

$$Z' = \int dq dp' dp_s ds s^{3N-1} \delta(H_N - E). \quad (19)$$

Integrating the irrelevant variable s using the fact that

$$\delta[F(s)] = \frac{\delta(s-s_0)}{F'(s)}, \quad (20)$$

where $F(s_0) = 0$, we find that

$$Z' = \int dq dp' d\xi \frac{Q}{gkT} \exp \frac{3N}{gkT} [E - H_0 - \frac{1}{2} Q\xi^2]. \quad (21)$$

From Eq. (21) we see that $g = 3N$ and $Q = 3NkT\tau^2$ where τ is some arbitrary time constant which governs the rate at which the equations of motion damp out fluctuations in the kinetic energy.

In our derivation we have considered the microcanonical ensemble rather than the molecular dynamics ensemble. We have not included considerations of momentum conservation. It is easy to see that $\Sigma \mathbf{p}_i$ is a constant of the motion generated by the Nose Hamiltonian. That \mathbf{p}_i is not a constant of the motion can be seen from the equivalent NH equations of motion.

In what follows we shall refer only to the NH form of the equations of motion. Henceforth, we will refer to \mathbf{p}_i' as \mathbf{p}_i . The NH equations of motion can be written in momentum conserving form as

$$\begin{aligned} \mathbf{q}_i &= (\mathbf{p}_i - \mathbf{p}_0)/m, \\ \dot{\mathbf{p}}_i &= \mathbf{F}_i - \xi (\mathbf{p}_i - \mathbf{p}_0), \\ \dot{\xi} &= \frac{1}{Q} \left[\sum \frac{(\mathbf{p}_i - \mathbf{p}_0)^2}{m} - 3(N-1)kT \right], \end{aligned} \quad (22)$$

where $\mathbf{p}_0 = \Sigma \mathbf{p}_i/N$ in which case the partition function is easily seen to be

$$Z = \int dq dp d\xi \exp -\beta(H_0 + \frac{1}{2} Q\xi^2) \quad (23)$$

with

$$Q = 3(N-1)kT\tau^2 \quad (24)$$

and

$$H_0 = \sum \frac{(\mathbf{p}_i - \mathbf{p}_0)^2}{2m} + \Phi(q). \quad (25)$$

In Fig. 1 we show computer simulation results for the distribution function $p(\xi)$. The system studied was 32 soft spheres $\phi(r) = 4\epsilon(\sigma/r)^{12}$ truncated at $r/\sigma = 1.5$. The state point simulated was $kT/\epsilon = 1.0$, $\rho\sigma^3 = 0.7$. The relaxation time τ [Eq. (24)] was taken to be $\tau(\epsilon/(m\sigma^2))^{1/2} = 0.09622$. This value was chosen because it is approximately equal to the Maxwell relaxation time (or "collision" time) τ_c for the system. Figure 1 shows that within statistical uncertainties ξ is distributed in a slightly skewed Gaussian fashion with a variance which agrees with the predicted value [Eq. (23)]. The thermodynamic properties of the NH simulation were also found to agree with estimates obtained using standard Newtonian molecular dynamics or Gaussian isothermal methods (see Sec. IV for further details).

III. NONEQUILIBRIUM PROPERTIES OF NH DYNAMICS

A. Equilibrium time correlation functions

We will now show that in the absence of external fields ($F_e = 0$) equilibrium time correlation functions computed by using the NH propagator or the Newtonian propagator are equivalent in the thermodynamic limit. Our method is essentially the same as that used by Evans and Morriss^{11,12} to show the thermodynamic equivalence of Gaussian isothermal and Newtonian equilibrium time correlation functions.

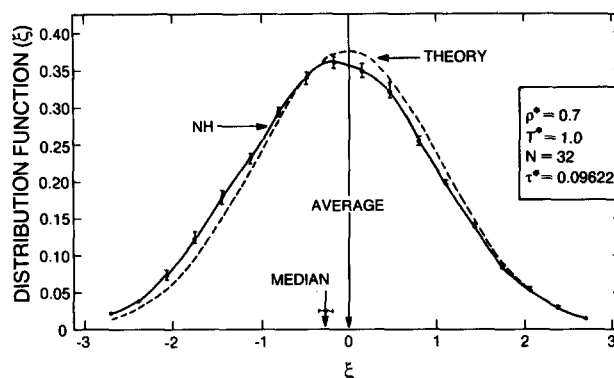


FIG. 1. This figure shows a comparison of predicted and observed distributions for ξ . The system studied was an equilibrium soft disk fluid.

One of the results which is central to the proof is the following. Consider a set of phase variables $\{U_\alpha\}$ whose equilibrium averages vanish

$$\langle U_\alpha \rangle_c = 0. \quad (26)$$

We will be interested in sets of local, extensive variables $U_\alpha = O(N)$. To be local and extensive we mean that firstly it is possible to decompose U_α into N formally identical intensive terms $U_{\alpha i}$,

$$U_\alpha = \sum_{i=1}^N \hat{U}_{\alpha i} \quad (27)$$

and secondly we require that

$$\langle \hat{U}_{\alpha i} \hat{U}_{\beta j} \rangle_c = 0 \text{ for all } \alpha, \beta, \text{ if } r_{ij} > r_c, \quad (28)$$

where r_c is some cutoff distance such as the range of the intermolecular potential.

If properties (26), (27), and (28) are satisfied then

$$\begin{aligned} \left\langle \prod_{\alpha}^M A_{\alpha} \right\rangle &= \sum_{i=1}^N \left\langle \hat{A}_{i1} \prod_{\alpha>1}^M A_{\alpha} \right\rangle \\ &= N \left\langle \hat{A}_{11} \prod_{\alpha>1}^M \left(\sum_{j, r_{1j} < r_c} \hat{A}_{\alpha j} \right) \right\rangle = O(N). \end{aligned} \quad (29)$$

Examples of zero mean, local, extensive variables are the fluctuations in the internal energy or the fluctuations in PV —the pressure tensor times the volume. Equation (29) shows that averages of products of such variables are extensive. The result can be generalized to include multiple time, correlation functions.

$$\left\langle \prod_{\alpha}^M A_{\alpha}(t_{\alpha}) \right\rangle = O(N). \quad (30)$$

The only difference in the proof being that the cutoff distance r_c must be increased to $r_c + c \text{Max}\{t_{\alpha}\}$ where c is the sound speed.

We will now use this result to compare equilibrium time correlation functions computed under Nose-Hoover and Newtonian dynamics.

Let

$$C(t_N) = \langle AB(t_N) \rangle_c = \langle A e^{iL_N t} B \rangle_c \quad (31)$$

denote a canonical ensemble time correlation function computed under Newtonian dynamics. Let $C(t_{\text{NH}})$ denote the corresponding function computed under Nose-Hoover dy-

namics [$F_e = 0$ in Eq. (8)]. We will drop the use of primes when describing NH momentum \mathbf{p}_i and rescaled NH time t' .

For such correlation functions to be of interest the phase variables A, B can be taken to be extensive but with zero mean. In most problems of interest they will also be local variables. Thus $C(t_N)$ and $C(t_{NH})$ are both extensive [$= O(N)$].

The difference between the two correlation functions $\Delta C(t)$ can be computed using the Dyson decomposition^{11,12} of propagators as

$$\Delta C(t) = \int_0^t ds \langle A e^{iL_N(t-s)} \Delta e^{iL_N s} B \rangle + O(\Delta^2), \quad (32)$$

where Δ , the difference between the respective Liouvillians is from Eq. (8) seen to be

$$\Delta = -\xi \sum \mathbf{p}_i \cdot \frac{\partial}{\partial \mathbf{p}_i} + \xi \frac{\partial}{\partial \xi}. \quad (33)$$

Normally phase variables of interest will not have any explicit dependence upon ξ and since the Newtonian Liouville operator is also independent of ξ , the last term in Eq. (33) can be ignored.

If B is an analytic function of momenta \mathbf{p}_i , it is clear that $\Sigma \mathbf{p}_i \cdot \partial / \partial \mathbf{p}_i$ will transform intensive variables into new intensive variables. Similarly it transforms extensive variables into new extensive variables. Thus,

$$\Delta C(t) = - \int_0^t ds \langle A (s_N - t_N) \xi B'(s_N) \rangle_c, \quad (34)$$

where B' is some new extensive variable.

From the equations of motion [Eq. (8)] and Eq. (24) for Q we see that ξ is intensive. This means that $\Delta C(t)$ is $1/N$ times the average of a product of 3 zero mean ($\langle A \rangle = \langle B' \rangle = \langle \xi \rangle = 0$), local extensive variables. Employing our lemma (30) concerning such products we see that

$$\Delta C(t)/C(t_N) = O(1/N). \quad (35)$$

B. Response theory

We will now consider the response of an NH system to an external field F_e . For simplicity we will assume that the external field is time independent. The equations of motion are

$$\begin{aligned} \dot{\mathbf{q}}_i &= \mathbf{p}_i/m + \mathbf{C}_i F_e, \\ \dot{\mathbf{p}} &= \mathbf{F}_i + \mathbf{D}_i F_e - \xi \mathbf{p}_i, \\ \dot{\xi} &= (K/K_0 - 1)/\tau^2. \end{aligned} \quad (36)$$

This is the external field form of the Nose-Hoover equations of motion for $\Sigma \mathbf{p}_i = 0$. The equation of motion for ξ has been obtained by substituting Eq. (24) into Eq. (22). The preset value of K is $K_0 = \bar{K} = 3NkT/2$. The variables \mathbf{C}, \mathbf{D} are phase variables which describe the coupling of the external field to the system. As usual we assume the adiabatic incompressibility of phase space or AIT . Thus

$$\sum \frac{\partial}{\partial \mathbf{q}_i} \cdot \mathbf{C}_i + \frac{\partial}{\partial \mathbf{p}_i} \cdot \mathbf{D}_i = 0. \quad (37)$$

A sufficient but not necessary condition for AIT is the existence of a Hamiltonian which could generate the adiabatic ($\xi = 0$) equations of motion.

It is convenient to define the dissipation functional J from the adiabatic derivative of the internal energy \dot{H}_0 :

$$\dot{H}_0^{\text{ad}} = J(\Gamma) F_e, \quad (38)$$

$$J = \sum \left(\frac{\mathbf{p}_i}{m} \cdot \mathbf{D}_i - \mathbf{F}_i \cdot \mathbf{C}_i \right).$$

We assume that at $t = 0$ a Nose-Hoover ensemble characterized by the N -particle distribution

$$f = \frac{\exp - \beta (H_0 + \frac{1}{2} Q \xi^2)}{\int d\Gamma \int d\xi \exp - \beta (H_0 + \frac{1}{2} Q \xi^2)} \quad (39)$$

is suddenly subject to a constant external field, F_e . We shall compute a formal expression for the N -particle response of the system. Now

$$f(t) = e^{-it} f_0, \quad (40)$$

where it is the f -Liouvillean:

$$\begin{aligned} iLA &= \left(\dot{\Gamma} \cdot \frac{\partial}{\partial \Gamma} + \xi \frac{\partial}{\partial \xi} \right) A + A \left(\frac{\partial}{\partial \Gamma} \cdot \dot{\Gamma} + \frac{\partial}{\partial \xi} \xi \right) \\ &= iLA + A\Lambda. \end{aligned} \quad (41)$$

L is called a p or phase Liouvillean and Λ is called the phase space compression factor since

$$(-1/f) df/dt = \Lambda.$$

The main trick that is required to convert Eq. (40) into a more useful form is to use of the Dyson equation to express the f propagator in terms of p propagators. Morriss and Evans recently proved the result¹² that

$$e^{-it} = \exp \left[\int_0^t ds \Lambda(-s) \right] e^{-iLs}. \quad (42)$$

Substituting this propagator transformation into Eq. (40) and using the fact that

$$iL [H_0 + \frac{1}{2} Q \xi^2] = JF_e - 3NkT\xi \quad (43)$$

we find

$$f(t) = \exp \left[\beta F_e \int_0^t ds J(-s) \right] f_0. \quad (44)$$

This is the Kawasaki form¹³ of the nonlinear response of the N -particle distribution function. Equation (44) for the Nose-Hoover response is the same formal expression as that for both the adiabatic and the Gaussian isothermal response. The only difference between the three cases is due to differences in the propagator used to generate $J(-s)$. In the present case it is the field dependent Nose-Hoover propagator.

Linearizing Eq. (44) and taking the average of an arbitrary zero mean phase variable B yields the usual Kubo form¹⁴ [Eq. (14)] for the linear response

$$\langle B(t) \rangle = \int_0^t ds \chi(s) F, \quad (45)$$

where

$$\chi(t) = \beta \langle B(t) J_0 \rangle. \quad (46)$$

In Eq. (46) the propagation is derived from the field free NH equations of motion (8). Thus the susceptibility $\chi(t)$ is given by an equilibrium time correlation function. The ensemble average is to be taken over the NH equilibrium ensemble

(23). This result is ergodically consistent because in an ergodic system time averaging of a single-phase trajectory will generate the entire equilibrium ensemble average.

Furthermore we know from Sec. III A and Eq. (35) in particular, that in the thermodynamic limit there is no difference between the susceptibility generated by NH dynamics and the corresponding ensemble of Newtonian trajectories. This means that in the thermodynamic limit the adiabatic (Newtonian), isothermal (Gaussian isothermal) and the Nose-Hoover *linear* responses are all equivalent. This is of course not true in the nonlinear regime.

IV. NUMERICAL COMPARISONS OF NON-NEWTONIAN MOLECULAR DYNAMICS ALGORITHMS

In Secs. II and III we have seen that NH dynamics yields correct predictions of the thermodynamic and linear transport properties of many-body systems. We decided to employ the NH thermostat to nonequilibrium molecular dynamics simulations of planar Couette flow. This would test the usefulness of the method in calculating the nonlinear transport properties of systems.

The method was tested by comparing it with the Gaussian isothermal, Gaussian isoenergetic and Berendsen schemes. The Gaussian schemes are well known from previous work and will not be further described here. The Berendsen method is very new and so we will give a very brief description.

It is basically a first order version of the NH scheme. The equations of motion are

$$\dot{\mathbf{q}} = \mathbf{p}_i/m, \quad (47)$$

$$\dot{\mathbf{p}}_i = \mathbf{F}_i - \xi \mathbf{p}_i, \quad (48)$$

$$\dot{\xi} = (K/K_0 - 1)/\tau.$$

The preset temperature T_0 is obtained from $K_0 = 3NkT_0/2$. The first thing to note about the Berendsen equations is that in contrast to all the Gaussian schemes and to NH dynamics, it is *irreversible*. This leads to profound theoretical difficulties when one tries to analyze either the equilibrium or nonequilibrium properties of Berendsen dynamics. As far as is known to the authors the form of its equilibrium distribution function is unknown as is the form of its linear response susceptibility. It is easily shown however that in contrast to all the Gaussian schemes and NH dynamics, that the canonical distribution function is *not* a solution of the Berendsen equations of motion.

A practical difficulty with the Berendsen equations is that they are very difficult to employ in nonequilibrium simulations at a specified state point. In the steady state the dissipation JF_e [Eq. (38)] must balance the energy removed by the thermostat $2K_{ss}\xi_{ss}$, thus

$$\langle J \rangle_{ss} F_e = \left\langle \frac{2}{\tau} K_{ss} \left(\frac{K_{ss}}{K_0} - 1 \right) \right\rangle. \quad (49)$$

Thus only at equilibrium when $F_e = 0$ does T_0 actually equal the temperature. In spite of these obvious difficulties we thought that a comparison with the Berendsen scheme might be useful in a practical demonstration of the essential independence of the computed properties to the details of the thermostating mechanism.

The system studied was the same as that employed in our earlier analysis of the ξ distribution at equilibrium. The 32 soft spheres were sheared using the now standard Slod algorithm.¹⁵ We have recently proved that under adiabatic conditions this algorithm correctly describes both the linear and nonlinear properties of Couette flow arbitrarily far from equilibrium.¹⁵

If we assume that a linear velocity profile is stable then thermostating is achieved in any of the various schemes by recognizing that

$$\left\langle \sum_i \frac{1}{2} m (\dot{\mathbf{q}}_i - i\gamma \mathbf{y}_i)^2 \right\rangle_{ss} = \frac{3}{2} NkT \quad (50)$$

provides a convenient definition of the temperature. In Eq. (50) γ is the shear rate $\partial u_x / \partial y$. The incorporation of Gaussian thermostats into the Slod equations for shear flow have been described many times before.¹²

Table I shows a comparison of the thermodynamic and transport properties for 32 soft spheres at a state point $kT/\epsilon = 1.0$, $\rho\sigma^3 = 0.7$, $\gamma\sigma(m/\epsilon)^{1/2} = 1.0$. It is important to realize that this state point is well into the Non-Newtonian regime with a shear viscosity which is only 71% of its Newtonian ($\gamma \rightarrow 0$) value. The hydrostatic pressure is approximately 5% greater than at equilibrium. Consequently the linear analysis of Sec. III is not useful in the theoretical interpretation of these results.

Table I shows results for NH simulations using three different values for τ ranging from approximately ten Maxwell relaxation ("collision") times (τ_c) down to $\tau_c/3$. For $\tau < \tau_c$ the equations of motion become stiff, requiring very short integration time steps. NH dynamics becomes very *inefficient* for small τ . From the table we see that for the run

TABLE I. This Table shows the comparative abilities of a number of different thermostats in maintaining shearing steady states. All units are reduced by the standard molecular parameters. The columns from left to right are: temperature, internal energy, shear viscosity, second moments of the internal energy and kinetic energy, the run length in 1000's of time steps and the integration time step. Note the greater efficiency of the two Gaussian methods. The reader can find a relative comparison of thermostats as applied to equilibrium systems in the review by Evans and Hoover (Ref. 16).

Method	kT/ϵ	E/ϵ	$\eta\sigma^2(m\epsilon)^{1/2}$	$(\Delta E/\epsilon)^2$	$(\Delta KE/\epsilon)^2$	kts	$\Delta(\epsilon/m\sigma^2)$
Gaussian isothermal	1.0	147.6 ± 0.1	1.524 ± 0.007	49.3 ± 10	0.0	50	0.003
Gaussian isoenergetic	$0.996 \pm .002$	147.38	1.537 ± 0.008	0.0	27.6 ± 2	40	0.003
NH $\tau(\epsilon/m\sigma^2)^{1/2} = 1$	$1.0001 \pm \pm 0.0002$	147.4 ± 0.2	1.55 ± 0.02	108.9 ± 2	60 ± 3	50	0.003
NH $= 0.09622$	0.998 ± 0.001	147.2 ± 0.2	1.56 ± 0.02	110 ± 4	52 ± 1	40	0.003
NH $= 0.0333$	0.998 ± 0.001	147.7 ± 0.4	1.56 ± 0.04	83 ± 3	43 ± 1	73	0.001
Berendsen $T_s = 0.78$	1.006 ± 0.003	148.4 ± 0.05	1.56 ± 0.03	62 ± 30	30 ± 10	60	0.003

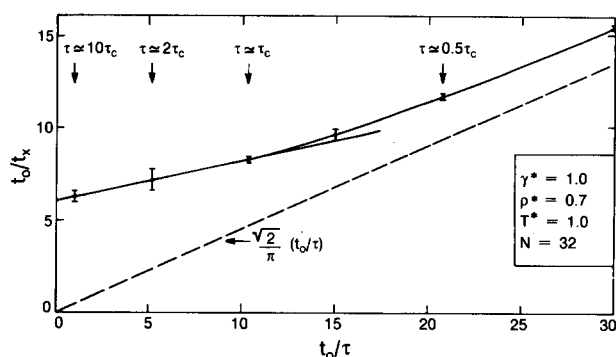


FIG. 2. This figure shows the mean kinetic crossing rate t_0/t_x as a function of the NH thermostating rate τ_0/τ . The system studied was the same as in Fig. 1 except that the fluid was subject to a reduced shear rate of unity. The solid curve gives the observed results while the dashed curve gives the results of a harmonic analysis of the corresponding ideal gas.

with $\tau(\epsilon/m\sigma^2)^{1/2} = 0.0333$, in spite of the fact that this run consumed the most computer time (73 000 time steps), it resulted in the poorest statistics for the computed shear viscosity. NH dynamics will also become inefficient γ is made too large since this will slow down the canonical averaging.

From the table one can see that the Gaussian methods are more than *twice as accurate* as any of the other methods which means that if all the methods were required to yield an accuracy of 1/2%, both of the Gaussian methods could achieve this target in less than 1/4 of the computer time required by any of the other methods.

All methods yield, within statistical uncertainties the same value of the shear viscosity. At present we have no theoretical understanding of why the properties of a nonlinear system should be so robust with respect to thermostating mechanism.

Finally, we were interested in investigating the effect of the Nose relaxation time τ , upon kinetic energy relaxation in nonequilibrium simulations such as shear flow. It is clear from the foregoing discussion that Gaussian and NH thermostating yield the same time averages and linear susceptibilities for variables which are not constants of the motion. It is not so clear, however, what the effect of temperature regulation will be upon kinetic energy relaxation. In Gaussian isothermal dynamics the kinetic energy is of course a constant of the motion. We might expect that in NH dynamics that the kinetic energy relaxation time will be roughly proportional to τ . It also seems plausible that this relaxation time will be shorter the further we move away from equilibrium.

We decided to examine the kinetic relaxation rate $\tau_k^{-1}(\tau^{-1})$, as a function of NH thermostating rate τ^{-1} . In particular can the kinetic relaxation rate be extrapolated back to its adiabatic value $\tau_k^{-1}(0)$, where the thermostating has been turned off? A more convenient statistic to gather in the NH-thermostated steady-shear experiments is the kinetic mean crossing time t_x defined as total trajectory time divided by the number of times that the kinetic energy K crosses its mean, or preset value $\bar{K} = K_0$; t_x is related to the correlation time by $t_x \sim 2\tau_K$.

In Fig. 2 we show the mean kinetic crossing rate t_x^{-1} , as a function of thermostating rate τ^{-1} for the NH-thermostated shear flow experiments. Notice that as the adiabatic limit

is approached—in particular for $\tau \gtrsim \tau_c$ (thermostating times larger than the equilibrium collision time)—the kinetic crossing rate is linear in the thermostating rate, with the adiabatic limit extrapolated to be $t_0/t_x \sim 6$; t_0 is the usual time unit $(m\sigma^2/\epsilon)^{1/2}$ (by comparison, $t_0/2\tau_c \sim 5$). For thermostating times shorter than the Maxwell time, equations of motion get stiffer and the kinetic crossing rate increases in a nonlinear fashion. There is some indication that as $\tau \rightarrow 0$, t_x^{-1} approaches a new linear regime with a higher slope of $\sqrt{2}/\pi$. In the ideal gas limit, harmonic analysis of the NH equations of motion [Eqs. (36)] yields $t_x^{-1} = (\sqrt{2}/\pi)\tau^{-1}$. In a sense, such a limit is achieved when $\tau \rightarrow 0$, since the momenta of particles change radically while their coordinates jiggle about essentially frozen positions. Hence, the magnitude of $\dot{\Phi}$ compared to \dot{K} is relatively small most of the time. It is interesting to note, however, that the $\tau \rightarrow 0$ limit of the NH equations of motion does *not* produce the isokinetic, or Gaussian thermostated results, since the NH kinetic energy fluctuations remain canonical (i.e., the kinetic heat capacity per particle is still $\frac{1}{2}k$), rather than approaching the isokinetic value, zero. This behavior is entirely analogous to the inability of classical statistical mechanics to give correct low temperature specific heats. In classical statistical mechanics each degree of freedom will remain equipartitioned no matter how high the characteristic frequencies become.

In conclusion, we have shown that the Nose-Hoover thermostat generates the canonical ensemble at equilibrium and gives correct linear nonequilibrium results which agree with other methods of thermostating. It also appears that in nonequilibrium steady states far from equilibrium, each of the thermostating algorithms discussed here yield essentially identical numerical results. We have no theoretical explanation for this. It also seems that of the methods studied here, the Gaussian isothermal method provides more efficient calculations of transport coefficients than the other methods. The Nose-Hoover and Berendsen algorithms allow the effects of thermostating to be extrapolated out of nonequilibrium molecular dynamics simulations so as to yield underlying adiabatic rates.

¹L. V. Woodcock, Chem. Phys. Lett. **10**, 257 (1971).

²D. J. Evans, J. Chem. Phys. **78**, 3297 (1983).

³H. C. Andersen, J. Chem. Phys. **72**, 2384 (1980).

⁴W. G. Hoover, A. J. C. Ladd, and B. Moran, Phys. Rev. Lett. **48**, 1818 (1982).

⁵J. M. Haile and S. Gupta, J. Chem. Phys. **79**, 3067 (1983).

⁶D. J. Evans and G. P. Morriss, J. Chem. Phys. **81**, 3749 (1984).

⁷H. J. C. Berendsen, J. P. M. Postma, W. F. van Gunsteren, A. Di Nola, and J. R. Haak, J. Chem. Phys. **81**, 3684 (1984).

⁸S. Nose, J. Chem. Phys. **81**, 511 (1984).

⁹S. Nose, Mol. Phys. **52**, 255 (1984).

¹⁰W. G. Hoover, Phys. Rev. A **31**, 1695 (1985).

^{10a}B. L. Holian and D. J. Evans, J. Chem. Phys. (to be published).

¹¹D. J. Evans and G. P. Morriss, Chem. Phys. **87**, 451 (1984).

¹²G. P. Morriss and D. J. Evans, Mol. Phys. **54**, 629 (1985).

¹³T. Yamada and K. Kawasaki, Prog. Theor. Phys. **38**, 1031 (1967).

¹⁴R. Kubo, J. Phys. Soc. Jpn. **12**, 570 (1957).

¹⁵D. J. Evans and G. P. Morriss, Phys. Rev. A **30**, 1528 (1984).

¹⁶D. J. Evans and W. G. Hoover, Annu. Rev. Fluid Mech. **18**, 243 (1985).